Hydrogen Storage

Nanoscaffold Mediates Hydrogen Release and the Reactivity of Ammonia Borane**

*Anna Gutowska, Liyu Li, Yongsoon Shin, Chongmin M. Wang, Xiaohong S. Li, John C. Linehan, R. Scott Smith, Bruce D. Kay, Benjamin Schmid, Wendy Shaw, Maciej Gutowski, and Tom Autrey**

The increasing demand for clean energy sources that do not add more carbon dioxide and other pollutants to the environment has resulted in increased attention worldwide to the possibilities of a "hydrogen economy" as a long-term solution for a secure energy future based on potentially renewable resources.[1–3] Some of the greatest challenges are the discovery and development of new on-board hydrogen-storage materials and catalysts for fuel-cell-powered vehicles. New materials that store both high gravimetric ($\geq 90\ gm\,H_2\,kg^{-1}$) and high volumetric ($\geq 82\ gm\,H_2\,L^{-1}$) densities of hydrogen that can be delivered at temperatures between −20 and 85 °C are needed by the year 2015.[4] The volumetric constraints eliminate from consideration pressurized hydrogen systems and guide towards the development of solid storage materials.[5] There are several broad classes of solid hydrogen-storage materials that are currently being investigated as potential on-board storage materials: 1) metal materials, hydrides (e.g., MgH_2),[6] imides (e.g., $LiNH_2$),[7] and organic frameworks (e.g., Zn_4O(1,4-benezenedicarboxylate)),[8] 2) complex hydrides (e.g., $NaAlH_4$),[9] and 3) carbon materials (e.g., carbon nanofibers,[10] single-wall carbon nanotubes).[11] The most thoroughly studied complex hydride, $NaAlH_4$, has been shown to release hydrogen at 110 °C when doped with Ti;[12] however, the kinetics are very slow and hydrogen-storage densities are too low ($56\ gm\,H_2\,kg^{-1}$) to meet long-term targets. The temperatures for H_2 release from carbon materials are too low, and the reported storage densities are controversial.[13] The hydrolysis of metal hydrides is being explored, but the unfavorable thermodynamics for regeneration of the spent material prevents their widespread application. For example, the reaction $NaBH_4 + 4\,H_2O \rightarrow NaB(OH)_4 + 4\,H_2$ is exothermic by $-250\ kJ\,mol^{-1}$. Reaction enthalpy for hydrogen loss is an important property since near-thermoneutral thermodynamics will be critical for materials for reversible H_2 storage. To date, few of these materials meet the long-term gravimetric requirements and provide rapid hydrogen release at temperatures between −20 and 85 °C; thus, new materials and novel approaches are needed. Herein we show that the kinetics of hydrogen release are significantly enhanced at low temperatures for a new hybrid material, ammonia borane infused in nanoporous silica, and that the hydrogen purity is increased. These findings suggest that hydrogen-rich materials infused in nanoscaffolds offer a most promising approach to on-board hydrogen storage.

Chemical hydrogen-storage materials that release H_2 by thermolysis without generating CO_2 may offer an attractive alternative to other systems studied. For example, the NH_xBH_x family of compounds[14] should provide favorable gravimetric densities of 245, 196, 140, and 75 $gm\,H_2\,kg^{-1}$ for $x = 4$, 3, 2, and 1, respectively. As the NB unit is isoelectronic with CC, these materials are viewed as inorganic analogues of hydrocarbons. However, NH_xBH_x compounds are solids rather than gases at ambient temperature because of their greater polarity and stronger intermolecular interactions relative to organic analogues. The inherent polarity results from the different electronegativities of the B and N atoms: 2.0 and 3.0, respectively.[15] As solids, they provide far more favorable volumetric densities than do the corresponding gaseous hydrocarbons. The two hydrogen-rich materials ammonium borohydride (NH_4BH_4) and ammonia borane (NH_3BH_3) were first prepared in the mid-1950s as part of the US government's program to develop boron-based jet fuels. NH_4BH_4 evolves hydrogen slowly at temperatures above −40 °C and thus is too unstable for applications at room temperature.[16] On the other hand, ammonia borane (AB) is a stable solid at room temperature and requires external heating to release H_2. AB decomposes upon melting at 114 °C with the vigorous bubbling of H_2 gas, or alternatively the hydrogen from AB can be released from the solid material at temperatures below 100 °C, albeit at significantly lower rates.[17] The thermal decomposition of NH_3BH_3 at temperatures below 100 °C yields H_2 and a complex polyaminoborane-like material $-(NH_2BH_2)_n-$ (PAB).[18] At temperatures above 150 °C the PAB decomposes to yield a second equivalent of H_2, concurrent with the formation of a further oxidized polyiminoborane-like material $-(NHBH)_n-$ (PIB) and borazine (c-$(NHBH)_3$).[19] The latter is an inorganic analogue of benzene that is highly undesirable in the H_2 feed.

Recent computational results indicate that the NH_xBH_x molecules also display favorable thermodynamics: All four consecutive steps of hydrogen release from NH_xBH_x for $x =$ 4–1 are thermoneutral to within $40\ kJ\,mol^{-1}$.[14,20] These theoretical results are supported by experimental work that shows that the reaction enthalpy for H_2 loss from NH_3BH_3 is only moderately exothermic ($\Delta H_{rxn} = -21\ kJ\,mol^{-1}$).[21] The

[*] Dr. A. Gutowska, Dr. L. Li, Dr. Y. Shin, Dr. C. M. Wang, Dr. X. S. Li, Dr. J. C. Linehan, Dr. R. S. Smith, Dr. B. D. Kay, Dr. W. Shaw, Dr. M. Gutowski, Dr. T. Autrey
Pacific Northwest National Laboratory
Richland, WA 99352 (USA)
Fax: (+1) 509-375-6660
E-mail: tom.autrey@pnl.gov
B. Schmid
University of Oregon
Department of Chemistry
Eugene, OR (USA)

[**] This research was performed in part at the Interfacial and Nano Science Facility in the William R. Wiley Environmental Molecular Sciences Laboratory, a national scientific user facility sponsored by the Office of Biological and Environmental Research of the US Department of Energy and located at the Pacific Northwest National Laboratory (PNNL). Pacific Northwest is operated for the Department of Energy by Battelle. The authors wish to acknowledge support from the Laboratory Directed Research and Development Program at the PNNL and the Nano Science & Technology Initiative. T.A. thanks D. Thorn (LANL) and D. Schubert (US Borax) for helpful discussions.

  DOI: 10.1002/anie.200462602

low reaction exothermicity of AB thermolysis is in significant contrast to hydrolysis pathways of boron-based hydrogen-storage materials. Given the approximate thermoneutrality of thermolysis accompanied by relatively low temperatures for H_2 release, AB is a strong candidate for on-board hydrogen storage. However, although AB exceeds targets for volumetric and gravimetric density for a hydrogen-storage material, three additional physical obstacles must be overcome: 1) The rates of H_2 release at temperatures below 85 °C must be increased, 2) borazine formation must be prevented, and 3) reversibility must be demonstrated.

There are reports that nanophase metal hydrides show enhanced kinetics for reversible hydrogen storage relative to the bulk materials.[22–24] However, after a few hydriding/dehydriding cycles the kinetic enhancement is diminished for some materials, as they lose nanophase structure.[25] Herein we suggest that a nanophase scaffold loaded with a hydrogen-rich material may provide an attractive option to preserve the nanoscale dimensions through several hydriding/dehydriding cycles. To demonstrate the effect of a nanophase scaffold on hydrogen release we use a high-surface-area mesoporous silica material loaded with AB as a model system. Three notable observations are described in this work: 1) increased rates of H_2 release, 2) modifications of the nonvolatile polymeric products that lead to a change in the thermodynamics of hydrogen release, and 3) minimized formation of borazine.

Mesoporous silica materials have an extremely high surface area and a highly ordered pore structure, which give them the appearance of nanochanneled silica scaffolds.[26] The mesoporous silica material used in this work, SBA-15, which was prepared according to a literature procedure,[27] is shown in Figure 1. The SBA-15 was loaded with AB by dosing the silica scaffold with a saturated methanolic solution of AB. Because of the porous nature of the silica scaffold, the internal channels of SBA-15 were filled rapidly by a capillary action directly upon exposure. The sample was dried under vacuum to remove the methanol and produce the SBA-15 coated with AB (1:1 by weight). Attempts to observe AB coated on the pores of SBA-15 by transmission electron microscopy (TEM) in ultramicrotome cross-sectional slices of the sample were not successful as a result of the weak scattering of electrons by the light elements B and N; however, electron dispersive spectrometry (EDS) of the microtome samples showed the presence of both elements B and N. Further evidence for the embedded material was inferred from BET measurements that show that the SBA-15 surface area is reduced from 900 $m^2 gm^{-1}$ before coating to $< 50\ m^2 gm^{-1}$ after coating.

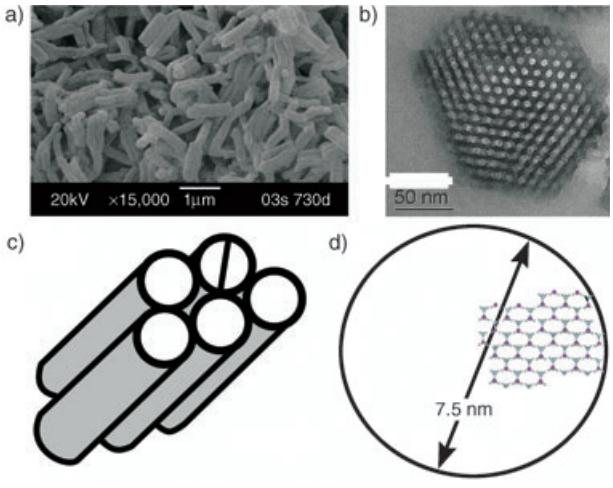

Figure 1. Schematic representation of AB in SBA-15, from the micro- to the nanoscale: a) SEM image of mesoporous silica; average particle size: 1 μm × 0.2 μm, surface area: ≈900 $m^2 gm^{-1}$, porous volume: 1.2 $mL g^{-1}$; b) TEM ultratome cross-sectional image of SBA-15 showing porous channels; c) schematic representation of parallel channels in SBA-15; pore diameter: 7.5 nm; d) schematic representation of a hydrogen-bonded AB network in the cross-section of a single pore.

Temperature-programmed desorption mass spectrometry (TPD/MS) was used to compare the temperature profiles of volatile products (H_2, borazine) released from neat AB and AB in the SBA-15 scaffold (Figure 2). Two peaks for neat AB

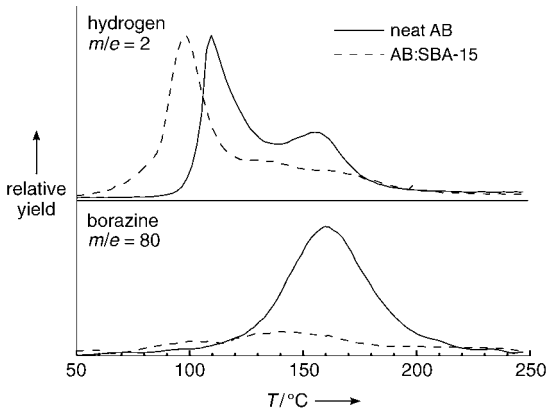

Figure 2. TPD/MS (1 °C min^{-1}) of volatile products generated by heating neat ammonia borane (solid line) and AB:SBA-15 (dashed line); $m/e = 2$ (H_2) and $m/e = 80$ (borazine, *c*-$(NHBH)_3$). The value $m/e = 2$ (H_2) is normalized to the area under the curve for neat ammonia borane (solid line). The corresponding scalar was used to normalize the $m/e = 80$ borazine data for AB:SBA-15.

at approximately 110 and 155 °C correspond to the release of the first equivalent of hydrogen with the formation of PAB, and the release of the second equivalent of hydrogen with the formation of PIB, respectively. There are two notable effects resulting from the nanostructure of AB in the SBA-15 scaffold: First, the temperature threshold for H_2 release ($m/e = 2$) is notably lower than the temperature threshold for neat AB, which is indicative of an enhanced rate of H_2 release. Second, the yield of the borazine side product ($m/e = 80$) is significantly lower than for neat AB. Solid-state ^{11}B NMR spectroscopy was used to analyze the nonvolatile products from neat AB and AB:SBA-15 to see if the borazine became entrapped within the mesoporous scaffold. However, no ^{11}B signal for borazine was observed, thus indicating that borazine is not likely to be trapped in the scaffold. Because borazine is not observed as a volatile product in the TPD/MS experiment and not detected by solid-state NMR spectroscopy, the mesoporous scaffold appears to affect the decomposition pathways of AB that lead to hydrogen formation.

Furthermore, if the PAB and PIB polymeric decomposition products formed in the SBA-15 scaffold do not form the more stabilized cyclization products, there may be a measurable difference between the reaction enthalpies for H_2 loss from AB:SBA-15 and neat AB.

Differential scanning calorimetry (DSC) experiments were used to quantify both the thermodynamics and kinetics for the release of the first equivalent of H_2 from neat AB and AB:SBA-15. Integration of the area under an isothermal DSC curve provides the enthalpy of reaction for H_2 release (ΔH_{rxn}). The enthalpy for H_2 loss from neat AB ($\Delta H_{rxn} = -21 \pm 1\ kJ\,mol^{-1}$) is in excellent agreement with the literature value for neat AB.[21] However, we find that the loss of H_2 from the AB in the scaffold is significantly less exothermic ($\Delta H_{rxn} = -1 \pm 1\ kJ\,mol^{-1}$). The difference in the observed ΔH_{rxn} for the release of H_2 from AB in the scaffold suggests that the nonvolatile products formed in the scaffold might be different from the nonvolatile products formed upon the release of H_2 from bulk AB. This hypothesis was confirmed by analysis of the ^{11}B NMR spectra of the nonvolatile products. After heating the 1:1 AB:SBA-15 mixture for 90 min at 85 °C only one resonance was observed (at $\delta = -23$ ppm), which we assign to PAB. On the other hand, after neat AB had been heated for 90 min at 85 °C three additional boron resonances were observed, as well as the PAB resonance.[28] The formation of the additional boron-containing products from neat AB must then contribute to the greater reaction exothermicity. The observation of a less exothermic enthalpy of reaction for H_2 loss from AB in the scaffold is important. As hydrogen loss becomes less exothermic, the reverse reaction, hydrogen uptake, becomes more favorable at a given pressure and temperature. The difference in the equilibrium between AB and PAB+H_2 in the neat material and the scaffold can be estimated from the van 't Hoff equation.[29] The experimental $\Delta\Delta H_{rxn}$ of 20 kJ mol^{-1} for H_2 loss from AB in the scaffold compared to H_2 loss from neat AB corresponds to a >4600-fold difference in pressure at room temperature!

The time dependence of H_2 release from neat AB at 80 °C and AB:SBA-15 at 50 °C is shown in Figure 3. The reaction exhibits sigmoidal kinetic behavior, and the extent of reaction (dashed curves) is indicative of an autocatalytic mechanism of hydrogen release.[30] The point ● on the integrated curve marks the half-life for hydrogen release. This analysis yields $t_{1/2} = 290$ min for the neat AB at 80 °C. The half-life for the 1:1 AB:SBA-15 sample at 80 °C could not be measured because the H_2 is released before the sample has reached this temperature ($t_{1/2} < 10$ min). However, if the temperature is decreased to 50 °C a baseline is observed for the AB:SBA-15 sample, and the kinetic analysis of the data results in a $t_{1/2}$ value of 85 min at 50 °C. Analysis of the integrated DSC data for various temperatures provides the half-life for hydrogen release as a function of temperature. Arrhenius treatment of this temperature-dependent rate data is shown in Figure 4. In both cases (neat AB and AB:SBA-15) a straight line is obtained; the gradient gives the apparent activation energy for hydrogen loss. These results suggest that the barrier for H_2 release from AB in the scaffold ($E_a \approx 67 \pm 5\ kJ\,mol^{-1}$) is significantly lower than the barrier for H_2 release from neat AB ($E_a \approx 184 \pm 5\ kJ\,mol^{-1}$). This large difference in activation energy manifests itself in a greater than 300-fold enhancement in the H_2-evolution rate at 70 °C. This result is important because one could potentially use the waste heat from a PEM (proton-exchange membrane) fuel cell (≈ 85 °C) to provide the heat to the hydrogen-storage media to drive hydrogen release.

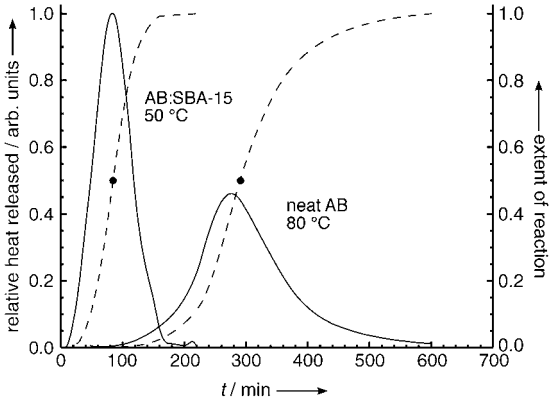

Figure 3. Scaled exotherms (solid lines) from isothermal DSC experiments that show the time-dependent release of H_2 from AB and AB:SBA-15 (1:1 wt/wt). The area under the curve for neat AB corresponds to $\Delta H_{rxn} = -21$ kJ mol^{-1}, and the area under the curve for AB:SBA-15 corresponds to $\Delta H_{rxn} = -1$ kJ mol^{-1}. The release of hydrogen from AB proceeds at a more rapid rate and at lower temperatures in SBA-15. The dashed line (——) is the integrated signal intensity; (●) is the point at which the reaction is 50% complete.

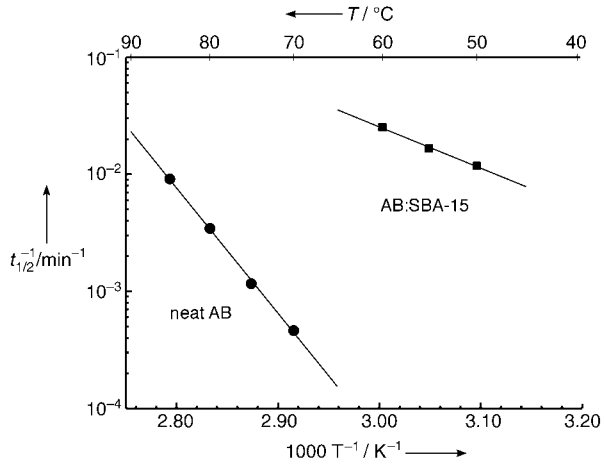

Figure 4. Arrhenius treatment of the temperature-dependent rate data yields a straight line with a gradient that is proportional to the apparent activation energy for hydrogen loss from neat AB (●; $E_a \approx$ 184 kJ mol^{-1}) or AB in the scaffold (■; $E_a \approx 67$ kJ mol^{-1}).

To our knowledge this is the first report of the use of an external agent (highly porous silica) to enhance the properties of a solid-state hydrogen-storage material. Coating the hydrogen-rich material AB within the mesoporus silica SBA-15 leads to: 1) suppression of borazine release, 2) modification of the enthalpy of the decomposition, and 3) lowering of the activation barrier for the loss of H_2. The enforced nanostructural geometry of the AB embedded in the scaffold may result in defect sites that initiate the dehydropolymeri-

zation reaction at lower temperatures. Alternatively, interfacial catalysis by the terminal SiO–H groups within the silica scaffold may result in the catalysis of the thermolysis of AB and control of the product distribution. These possibilities will be explored in forthcoming studies. The results for AB in the mesoporous silica are notable in themselves. We believe, however, that mesoporous materials may improve the kinetics and thermodynamics of hydrogen release from other materials, such as hydrogenated metal nitrides and imides or $LiBH_4$. For example, it has recently been reported that SiO_2 powder lowers the onset temperature for hydrogen release from $LiBH_4$.[31] The high surface area of SBA-15 would probably have very similar benefits and could enhance the kinetics for rehydriding, as the $LiBH_4$ would be confined to a nanophase structure.

Experimental Section

SBA-15 synthesis: Hexagonally ordered mesoporous silica (SBA-15) was prepared according to published procedures.[32] In a typical preparation of mesoporous silica with pores of 100 Å in diameter, pluronic P123 ($\bar{M}_W = 5800$; 12.0 g) was dissolved in 2 M HCl (360 mL) at 40 °C. Tetraethylorthosilicate (TEOS; 25.5 g) was added to the resulting milky solution, which was then stirred for 18 h at the same temperature. The mixture was transferred into a teflon-lined autoclave and heated at 100 °C for 24 h without stirring. The white precipitate was filtered, dried in air, and finally calcined at 550 °C for 6 h.

Preparation of AB:SBA-15: A solution of AB (50 mg) in methanol (300 μL) was added to a sample of SBA-15 (50 mg). The methanolic solution appeared to fill the internal channels of the mesoporous scaffold through a capillary action. The "wet" SBA-15 was dried under vacuum to produce a sample with an internal coating of ammonia borane (approximately 1:1 AB to SBA-15 by weight).

TEM: A thin section of the specimen was prepared for high-resolution TEM (HRTEM) by standard epoxy embedding followed by ultramicrotoming to a thickness of less than 50 nm. The HRTEM analysis was carried out with a Jeol JEM 2010 microscope with a specified point-to-point resolution of 0.194 nm. The operating voltage of the microscope was 200 keV. All images were recorded digitally with a slow-scan CCD camera (image size: 1024×1024 pixels), and image processing was carried out by using a digital micrograph (Gatan).

DSC/TPD/MS: DSC analyses were performed by using a Netzsch STA 409 TGA/DSC and a Pfeiffer QMS300 MS or a Setaram C80 calorimeter. The TPD/MS data for $m/e = 2$ (H_2) and $m/e = 80$ (borazine) were obtained by monitoring the off-gas with a heated fused (200 °C) silica capillary (a 1-m silanized fused silica capillary, 0.1 mm ID) attached to the top of the Netzsch instrument. The MS uses a standard electron impact ionization detector. The MS scanning rate was 12 s for a range of 1 to 100 amu. To obtain the relative yields of hydrogen and borazine, samples of AB (6.2 mg) and SBA-15:AB (1:1 wt/wt; 6.2 mg) were weighed into a Pt crucible for back-to-back experiments. The area under the SBA-15:AB curve was multiplied by a factor of two to provide a direct comparison for H_2 and borazine release from neat AB and AB embedded into the SBA-15 scaffold. A thermal ramp of 1 °C min^{-1} from room temperature to 200 °C with an argon flow of 20 $cm^3 min^{-1}$ were used in our analysis.

^{11}B NMR spectroscopy: Spectra of amino borane samples were recorded on a Varian Unity Inova spectrometer operating at a ^1H frequency of 800 MHz with a 4-mm 3-Ch Doty MAS probe. For the Bloch decay experiment a 200-kHz sweep width, a 5-μs 90°-pulse for ^{11}B (with and without ≈ 30 kHz decoupling), and a pulse delay of 5 s were used. Samples were spun at 15 kHz then cooled to 10–20 °C, and 128 scans were collected for each spectrum.

Received: November 13, 2004
Published online: May 4, 2005

Keywords: hydrogen storage · kinetics · mesoporous materials · nanostructures · thermochemistry

[1] P. Grant, *Nature* **2003**, *424*, 129–130.
[2] M. S. Dresselhaus, I. L. Thomas, *Nature* **2001**, *414*, 332–337.
[3] L. de Palacio, P. Busquin, Report from Europa Commission, "Hydrogen Energy and Fuels Cells: A Vision for Our Future", http://europa.eu.int/comm/research/energy/nn/nn_rt/nn_rt_hlg/article_1146_en.htm.
[4] Recent information can be found at: http://www.eere.energy.gov/hydrogenandfuelcells/pdfs/freedomcar_targets_explanations.pdf.
[5] W. Grochala, P. P. Edwards, *Chem. Rev.* **2004**, *104*, 1283–1316.
[6] J. Huot, J. F. Pelletier, G. Liang, M. Sutton, R. Schultz, *J. Alloys Compd.* **2002**, *330–332*, 727–731.
[7] P. Chen, Z. Xiong, J. Luo, J. Lin, K. L. Tan, *Nature* **2002**, *420*, 302–304.
[8] N. L. Rosi, J. Eckert, M. Eddaoudi, D. T. Vodak, J. Kim, M. O'Keeffe, O. M. Yaghi, *Science* **2003**, *300*, 1127–1129.
[9] L. Schlapbach, A. Zuttel, *Nature* **2001**, *414*, 353–358.
[10] D. J. Browning, M. L. Gerrard, J. B. Lakeman, I. M. Mellor, R. J. Mortimer, M. C. Turpin, *Nano Lett.* **2002**, *2*, 201–205.
[11] A. C. Dillon, K. M. Jones, T. A. Bekkedahl, C. H. Kiang, D. S. Bethune, M. J. Heben, *Nature* **1997**, *386*, 377–379.
[12] K. J. Gross, G. J. Thomas, C. M. Jensen, *J. Alloys Compd.* **2002**, *330*, 683–690.
[13] G. B. Tibbetts, G. P. Meisner, C. H. Olk, *Carbon* **2001**, *39*, 2291–2301.
[14] M. Gutowski, T. Autrey, J. Linehan, unpublished results.
[15] L. Pauling, *General Chemistry*, Dover Publications, New York, **1988**, p. 182.
[16] R. W. Parry, D. R. Schultz, P. R. Girardot, *J. Am. Chem. Soc.* **1958**, *80*, 1–3.
[17] J. Baumann, Dissertation, Physikalisch-chemische Untersuchungen zur Wasserstoffabgabe von BNH-Verbindungen, **2003**, TU-Bergakademie Freiberg, Germany. The research group in Freiberg has been investigating NH_3BH_3 as a hydrogen-storage material.
[18] F. Baitalow, J. Baumann, G. Wolf, K. Jaenicke-Rößbler, G. Leitner, *Thermochim. Acta* **2002**, *391*, 159–168.
[19] V. Sit, R. A. Geanangel, W. W. Wendlandt, *Thermochim. Acta* **1987**, *113*, 379–382.
[20] M. Gutowski, T. Autrey, *Prepr. Pap. Am. Chem. Soc. Div. Fuel Chem.* **2004**, *49*, 275–276.
[21] G. Wolf, J. Baumann, F. Baitalow, F. P. Hoffmann, *Thermochim. Acta* **2000**, *343*, 19–25.
[22] J. Liang, *Prepr. Pap. Am. Chem. Soc. Div. Fuel Chem.* **2003**, *48*, 281–283.
[23] H. Fujii, S. Orimo, *Phys. B* **2003**, *328*, 77–80.
[24] W. Oelerich, T. Klassen, N. Eigen, R. Bormann, *EUROMAT* **2000**, *13*, 141–145.
[25] Y. Suzuki, T. Haraki, H. Uchida, *J. Alloys Compd.* **2002**, *330–332*, 488–491.
[26] D. Zhao, J. Feng, Q. Huo, N. Melosh, G. H. Fredrickson, B. F. Chmelka, G. D. Stucky, *Science* **1998**, *279*, 548–552.
[27] Y. Shin, J. Liu, L.-Q. Wang, Z. Nie, W. D. Samuels, G. E. Fryxell, G. J. Exarhos, *Angew. Chem.* **2000**, *112*, 2814–2819; *Angew. Chem. Int. Ed.* **2000**, *39*, 2702–2707.
[28] The 800-MHz solid-state NMR spectrum is available as Supporting Information. Observed ^{11}B resonances: AB:SBA-15

(one signal, $\delta = -23$ ppm), neat AB (four signals, $\delta = -6$, -12, -23, -37 ppm).

[29] van 't Hoff equation: $\ln(p_{eq}/p^{o}_{eq}) = \Delta H/RT - \Delta S/R$. The difference in hydrogen overpressure can be calculated from $\Delta\Delta H$ of H_2 loss from AB bulk and AB in the scaffold. $\Delta\ln(p_{eq}/p^{o}_{eq}) = \Delta\Delta H/RT - \Delta\Delta S/R$. $\Delta\Delta S = 0$, $\Delta\Delta H = 20\ kJ\,mol^{-1}$, then $p_{eq}(AB)/p_{eq}(AB{:}SBA\text{-}15) = 4667$. As $\Delta H \approx 0$ in the scaffold, the pressure required for H_2 uptake by the spent AB is the pressure required to overcome the entropy of formation of the gaseous H_2. Reversibility processes will be addressed in a subsequent publication.

[30] For similar observations with $LiBH_4$ and triethanolamine, see: R. Custelcean, J. E. Jackson, *J. Am. Chem. Soc.* **2000**, *122*, 5251 – 5257.

[31] A. Zuttel, P. Wenger, P. Sudan, P. Mauron, C. Emmenegger, *J. Power Sources* **2003**, *118*, 1 – 7.

[32] D. Zhao, Q. Huo, J. Feng, B. F. Chmelka, G. D. Stucky, *J. Am. Chem. Soc.* **1998**, *120*, 6024 – 6036.

